

## Research Article

# Electrooxidation and Development of a Highly Sensitive Electrochemical Probe for Trace Determination of the Steroid 11-Desoxycorticosterone Drug Residues in Water

Wejdan T. Alsaggaf and Mohammad S. El-Shahawi 

Department of Chemistry, Faculty of Science, King Abdulaziz University, P.O. Box 80203, Jeddah 21589, Saudi Arabia

Correspondence should be addressed to Mohammad S. El-Shahawi; [mohammad\\_el\\_shahawi@yahoo.co.uk](mailto:mohammad_el_shahawi@yahoo.co.uk)

Received 16 January 2022; Revised 10 March 2022; Accepted 4 April 2022; Published 4 May 2022

Academic Editor: Rajan Jose

Copyright © 2022 Wejdan T. Alsaggaf and Mohammad S. El-Shahawi. This is an open access article distributed under the Creative Commons Attribution License, which permits unrestricted use, distribution, and reproduction in any medium, provided the original work is properly cited.

Anabolic-androgenic steroids (AASs), a class of compounds frequently misused by competitors and unfortunately by the general population, have lately attracted international attention. Thus, extraordinary demands for developing low cost, precise, rapid, and facile protocols for detection and/or determination of AAS have arisen. Hence, the current strategy explores for the first time the redox features of 21-hydroxypregn-4-ene-3, 20-dione, namely, 11-desoxycorticosterone (DCS) AA drug steroid at a glassy-carbon electrode (GCE) in a wide pH range (pH 2.0–10.0) by adsorptive differential pulse-anodic stripping voltammetry (DP-ASV) and cyclic voltammetry (CV). At pH 2, DP-ASV and CV at the optimized pH 2–3 displayed an irreversible anodic peak at 0.4 V versus Ag/AgCl electrode. The dependency of the anodic peak current of the CV at 0.4 V at various concentrations and scan rate of the DCS drug was characteristic of an electrode-coupled electron transfer of EE type mechanism. At the optimized parameters, the proposed strategy allowed quantification of DCS in the concentration range 2.5–13.19 nM (0.83–4.36 ng mL<sup>-1</sup>) with satisfactory limits of detection (LOD) and quantization (LOQ) of  $9.3 \times 10^{-1}$  nM ( $3.1 \times 10^{-1}$  ng mL<sup>-1</sup>) and 3.1 nM (1.02 ng mL<sup>-1</sup>), respectively. A relative standard deviation (RSD) of  $\pm 3.93\%$  ( $n = 5$ ) at 4.0 ng mL<sup>-1</sup> DCS was achieved. The established probe was fruitfully employed and validated for trace determination of DCS residues in environmental water. The interference of several common diverse species on DCS sensing was insignificant revealing good selectivity. The established probe exhibited good sensitivity, selectivity, precision, and accuracy, short analytical time, and low cost compared with the reported methods, for DCS determination.

## 1. Introduction

Nowadays, the routine usage of anabolic-androgenic steroids (AASs) as drugs to increase the human performance is well known in sport activities [1]. With the growing use of ASs, their side effects have also become a reason of alarm [2]. The presence of various levels of double and triple bonds in addition to other functional groups in ring substituents of anabolic steroids is responsible for their great diversity [3, 4]. Designed medical drugs, e.g., anabolic steroids (AS), have been used to treat depression in 1930s [5]. AASs are involved in the regulation of different physiological processes in males and could treat hormonal problems, e.g., delayed puberty and diseases, that lead to muscle loss, including cancer,

AIDS, and therapeutic purposes, including antiasthmatics, bronchodilators, and tocolytics as repartitioning agent [6, 7]. Synthetic and natural steroids have been also used as growth promotion and feed conversion efficiency in animals [8]. Thus, there is a need to create simple, quick, and delicate protocols for detection of these chemicals in environmental samples [9].

Recently, researchers have reported a strong correlation between breast cancer development and increase levels of circulating steroid presented in estrogens in the body [10]. Thus, the use of exogenous steroids such as androgenic, estrogenic, or progestagenic activity and thyrostatics in meat or milk has been prohibited by the European Union (EU) and China [10, 11]. On the other hand, anabolic steroids

have been used as doping agents in the sport field, due to their preferable effects among the so-called body builders and weight fighter [12] and subsequent release from biological fluids such as urine into the aquatic environment [12, 13]. Most of the societies have considered anabolic steroids as drug abuse chemicals, duly important and crucial to the human health similar to opiates and alcohols [14]. Hence, great concern for environmentalists has been oriented towards developing reliable and low-cost methods for rapid detection and quantification of anabolic steroids at trace levels because of their emerging issue in water and biological fluids [15, 16].

Numerous chromatographic techniques, e.g., use of aptamer combined with microtiter plate assay against the AAs [9, 15–17], thin-layer chromatographic analysis [18], QuEChERS and ultra-high performance liquid chromatography tandem mass spectrometry, and HPLC/MS/MS [19–24] and gas chromatography and GC/MS [25–27] have been reported for DCS detection at trace levels. The need of derivatization, sophisticated instrumentation, high running cost, time-consuming, use of large amounts of toxic organic solvents in the extraction step, and sample pretreatment of these complex methodologies are the main drawbacks that make them unfeasible for routine analysis [20, 23–26]. Most of these sophisticated high-end techniques are also not appropriate for measuring trace levels of the entitled drug, significant loss of anabolic steroids remains, and there is a need for well skilled personnel for proper operation of these techniques [21–25]. Moreover, separation/preconcentration of target analyte can minimize these drawbacks prior to its determination [22–25]. Thus, there is an immense need to develop a low-cost electrochemical sensor as a potential facile alternative for rapid and precise detection of trace-level levels of this class of chemicals in pharmaceutical formulations and water samples of complex matrices [28, 29]. Electrochemical voltammetric methods have been less approached compared to colorimetric or chromatographic assays, so the development of electrochemical probes may represent great interest for the rapid and specific detection of the entitled drug [29].

In today's era, electrochemical techniques based on nonmodified and surface modified electrode (SME) have gained wide recognition in rapid and trace determination of (bio)-chemical analytes such as 17  $\beta$ -estradiol and other steroids [28–35]. The anabolic steroid *21-hydroxypregn-4-ene-3, 20-dione known as 11-desoxycorticosterone* (Supplementary information's, ESI-1) has been extensively used due to its unlimited aptitude to motivate protein synthesis and improve compensatory adaptation in the humans [2, 10]. To the best of our knowledge, the current study represents the first report on the electrochemical oxidation of the entitled drug (ESI. 1) based on its strong affinity towards GCE. On the other hand, the DP-ASV of the DCS at bare GCE provided stable and reproducible signals that can be used for DCS detection. The DP-ASV approach is simple, easy to use, and of low cost. This approach also provides low capacitive current combined with a great discrimination of faradaic current that it can improve the sensitivity and affinity towards DCS. Based on this information, the purpose of the

present study is focused on (i) understanding the kinetics and electrode mechanism of the entitled DCS steroid at the bare GCE; (ii) studying the sensitivity and performance of the developed anodic peak at GCE towards determination of the entitled drug (DCS); and finally (iii) applying the established DP-ASV method for detection of DCS residues in water samples.

## 2. Experimental

**2.1. Reagents and Materials.** Analytical-reagent grade (A.R) chemicals and solvents were used as received. All glassware including electrochemical cell and high density polyethylene (HDPE) bottles (Nalgene) was precleaned by soaking in HNO<sub>3</sub> (10% v/v), washed with deionized water, hot detergent, soaked in 50% HCl (Analar), HNO<sub>3</sub> (2.0 M), rinsed with water, and finally dried in an oven at 80°C. HDPE bottles were used for storing the samples. The steroid 11-desoxycorticosterone (DCS) IUPAC, named as 21-hydroxypregn-4-ene-3, 20-dione (ESI. 1) (99%, HPLC), was purchased from Sigma-Aldrich (Steinheim, Germany). A stock solution of DCS ( $1.0 \times 10^{-3}$  M) in methanol was prepared and stored at  $-18^\circ\text{C}$  for no longer than six months. Standard DCS working solutions ( $3.3 \times 10^{-6}$  –  $6.0 \times 10^{-5}$  M) of the drug were prepared in ultra-pure water and stored at  $4^\circ\text{C}$  for no longer than one week for use. A series of Britton-Robinson (B-R) solutions (pH 1.96–10.0) were prepared as reported [36]. Various solutions of pH 1.41–1.8 were also prepared from dilute HCl at different concentrations (0.05–0.1 M) to study the impact of the acidity on the redox characteristics of the entitled drug.

**2.2. Instrumentation.** A Metrohm 757 VA trace analyzer and 747 VA stand (Basel, Switzerland) were used for recording the cyclic voltammetry (CV) and differential pulse-anodic stripping voltammetry (DP-ASV). A three-compartment borosilicate (Metrohm) voltammetric cell (10 mL) configuration incorporated Bioanalytical System bare GCE (diameter = 2 mm) as a working electrode, double-junction Ag/AgCl ( $3.0 \text{ mol L}^{-1}$ ), KCl as a reference, and Pt wire (BAS model MW-1032) as counter electrodes, respectively. Digital-micropipettes 10–1000  $\mu\text{L}$  (Volac) were used for the preparation of more diluted standard solutions. A “tangent fit method” was used for measuring the peak current heights. A Metrohm pH-meter (Basel, Switzerland) and Milli-Q Plus system (Millipore, Bedford, MA, USA) were used for measuring the solution pH and for providing Milli-Q water throughout the work, respectively.

**2.3. Recommended DP-ASV Procedures for DCS Determination.** The electrochemical cell was precleaned by soaking in nitric acid (10% v/v) and washed with deionized water. Bare GCE (diameter: 2 mm) was polished with 0.05 mm alumina slurry to a mirror finish, rinsed thoroughly with 1:1 HNO<sub>3</sub>–H<sub>2</sub>O (v/v), washed with pure ethanol and redistilled water, and finally dried. The following procedures were then performed using precleaned GCE as follows: an accurate volume (10.0 mL) of B-R buffer (pH 2) as a

supporting electrolyte was transferred into the voltammetric cell containing precleaned GCE as working, double-junction Ag/AgCl ( $3.0 \text{ mol L}^{-1}$ ), KCl as a reference, and Pt wire as counter electrodes, respectively. The test solution was then stirred and purged with  $\text{N}_2$  gas for 15 min before recording. The stirrer was stopped, and after 10 s equilibrium time, the background DP-ASV of the supporting electrolyte was recorded by applying a positive going potential from  $-1.0$  to  $+1.5 \text{ V vs. Ag/AgCl}$  electrode at the optimized analytical parameters of deposition potential ( $0.007 \text{ V}$ ); accumulation time ( $5 \text{ s}$ ); pulse amplitude ( $70 \text{ mV}$ ) and  $70 \text{ mV s}^{-1}$  scan rate. After recording the DP-ASV of the supporting electrolyte solution, known concentrations ( $3.3 \times 10^{-6}$ – $6.0 \times 10^{-5} \text{ M}$ ) of DCS were introduced into the electrochemical cell. The solution was stirred for 5 min and purged with  $\text{N}_2$  after each addition of DCS. The stirrer was then stopped and after 10 s equilibrium time, the DP-ASV of DCS was finally recorded by applying the same positive going potential ( $-1.0$  to  $1.5 \text{ V}$ ) under the optimized parameters of the supporting electrolyte solution. The corresponding anodic peak current of the DP-ASVs at  $0.40 \text{ V vs. Ag/AgCl}$  was finally measured after correction of the background current of the blank. The results were further used for construction of the calibration plot, and the DCS concentration was calculated via the standard calibration curve.

The impact of DCS concentrations ( $1.0 \times 10^{-4}$ – $5.0 \times 10^{-4} \text{ M}$ ) at various scan rate ( $20$ – $100 \text{ mV/s}$ ) was further studied by cyclic voltammograms at the optimized pH 2 at bare GCE to assign the electrode mechanism. The cell and electrodes were washed with deionized water and installed in the blank solution after each measurement, and the CV of the blank solution was also recorded successively for 30 cycles for renewing the surface of the bare GCE.

**2.4. Analytical Applications and Validations of the Established DP-ASV Methodology.** HDPE was subjected to  $\text{HNO}_3$  ( $10\%$ , v/v) solution overnight washing period and rinsed with deionized water prior to its use. Tap water sample (approximately  $200 \text{ mL}$ ) was collected in HDPE bottles from a domestic tap from Chemistry laboratory, King Abdulaziz University, Jeddah, Saudi Arabia, which was left to run for  $20$ – $25 \text{ min}$  prior sampling. The water sample was filtered through  $0.45 \mu\text{m}$  pore size cellulose membrane filter (Millipore Corporation) and stored in LDPE sample bottles at  $4^\circ\text{C}$ . A known volume ( $5.0 \text{ mL}$ ) of the prefiltered water sample was transferred to the cell in the presence of B-R buffer solution ( $5.0 \text{ mL}$ , pH 2) as a supporting electrolyte. Under the optimized parameters used for construction of the DP-ASV calibration curve, the Ads-DPVs were recorded in the absence and after addition of standard fractions ( $20.0$ – $100 \mu\text{L}$ ) of DCS ( $5.0 \times 10^{-6} \text{ M}$ ). The corresponding anodic peak current ( $i_{p,a}$ ) of each individual solution was subsequently measured at  $0.40 \text{ V versus Ag/AgCl}$  electrode. The unknown DCS concentration was then determined from the regression equation of the linear calibration plot. On the other hand, the standard addition method was also performed by measuring the anodic peak current in the absence and presence of known fractions ( $20.0$ – $100 \mu\text{L}$ ) of known

concentrations of DCS under the optimized parameters. The DCS concentration was then determined via extrapolated abscissa of the linear plot of the standard addition using the following equation [37]:

$$[\text{DCS}] = [\text{Cs}] \times \frac{(i_{p,a})_{(\text{samp})}}{(i_{p,a})_{(\text{stand})}}, \quad (1)$$

where  $[\text{C}_{\text{stand}}]$  is the standard DCS concentration, and  $(i_{p,a})_{\text{samp}}$  and  $(i_{p,a})_{\text{stand}}$  are the anodic peak currents displayed by the sample and after addition of the standard DCS in  $\mu\text{A}$ , respectively. The calculated recovery percentages via the standard addition plot at room temperature ( $\sim 25^\circ\text{C}$ ) were further used for assigning the precision, accuracy, and validation of the proposed method. The electrochemical measurements were performed at room temperature ( $\sim 25^\circ\text{C}$ ).

### 3. Results and Discussion

The selection of the working electrode in stripping voltammetry is vital, since its performance in developing highly sensitive method for analyzing the target compound depends on its adsorption and interaction with the electrode surface. Thus, the interaction of the DCS with the non-modified electrode, e.g., glassy carbon electrode (GCE), carbon paste (CP), and Au, was studied. Preliminary screening of cyclic voltammetry of the DCS drug at GCE, Au, and CPE as a working electrode revealed strong interaction of the drug towards GCE. On the other hand, the low cost and the availability of the bare GCE in addition to its high affinity and interaction with the target DCS drug compared to other nonmodified Au and CPE electrodes suggested its use as a working electrode in DP-ASV for detection of trace levels of DCS in water samples. This study at GCE signifies the first report on the redox behavior of the DCS drug. Thus, the redox behavior of the entitled drug was critically studied below.

**3.1. Electrochemical Oxidation of DCS at GCE.** The impact of pH of the electrolysis medium and the interaction of the DCS drug towards bare GCE represent the main important parameters that control the shape of the DP-ASV, peak potential, peak current, and sensitivity. Thus, the DP-ASVs of the DCS at the bare GCE were recorded over a wide range of B-R buffer (pH  $2.0$ – $9.01$ ) as supporting electrolyte in the potential range  $-0.5$ – $1.0 \text{ V vs. Ag/AgCl}$  electrode.

The DP-ASVs of the supporting electrolytes at the employed pH range revealed no signals whereas, in the presence of DCS ( $2.5 \times 10^{-6} \text{ M}$ ), and the DP-ASVs of one well-defined anodic peak in the potential range  $0.30$ – $0.40 \text{ V}$  was observed depending on the solution pH. Representative results are shown in Figure 1. Upon raising the solution pH, the potential of the anodic peak was shifted to more positive values revealing the involvement of proton/electron transfer [38]. The data also confirm the irreversible nature of the electrochemical oxidation process and the dissociation of the DCS before the rate-determining step [38, 39]. Thus, the observed anodic peak is most likely attributed to the

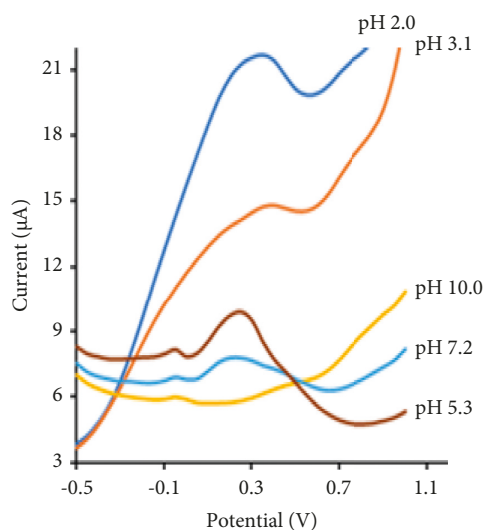


FIGURE 1: Ads -DP-ASVs of various B-R buffer solutions of pH $\approx$ 2–9.01 in the presence of DCS (10 nM) at GCE vs. Ag/AgCl electrode. Scan rate = 100 mVs<sup>-1</sup>, deposition time = 60 s and 0.07 V deposition potential.

electrochemical oxidation of the hydroxyl group (-C-OH) of the DCS to the corresponding carbonyl group (-C=O) as shown in Scheme 1 as reported earlier [31, 32].

At various concentrations of HCl (pH 1.4–3.0) as a supporting electrolyte, the DP-ASV was further studied. At the studied pH ranges of pH 1.4–3.0 and pH 2.0–9.02 using HCl and B-R buffer solutions (0.1 M), the DP-ASVs were recorded in the presence of DCS ( $8.0 \times 10^{-6}$  M). The plot of the anodic peak current ( $i_{p,a}$ ) of the DP-ASVs vs. pH is shown in Figure 2. The DP-ASV displayed one well defined anodic in the potential range 0.30–4.0 V vs. Ag/AgCl electrode, where the maximum anodic peak current was achieved at pH 2–3 in B-R buffer as supporting electrolyte. The observed oxidation peak at  $E_{p,a} = 0.402$  at pH 2–3 was well defined, symmetric, and reproducible; thus, in the succeeding study, the solution pH was adopted at pH 2–3 using B-R buffer where at this pH better stability and reproducibility of the peak current was noticed.

The CVs of DCS ( $1.50 \times 10^{-3}$  M) at various scan rate (20–100 mV/s) were individually recorded on freshly polished GCE in B-R buffer solution of pH 2–3 vs. Ag/AgCl electrode. Representative results are demonstrated in Figure 3. The CVs showed one well-defined anodic peak and one ill-defined cathodic peak in the potential window -1.5 to +1.5 V vs. Ag/AgCl electrode. On reversing the scan, an ill-defined cathodic peak potential ( $E_{p,c}$ ) at -0.5 to -0.6 V was observed at all scan rates, adding further support to the irreversible nature of the electrochemical oxidation process. The anodic peak potential ( $E_{p,a}$ ) was shifted to more positive values, whereas the  $E_{p,c}$  of the cathodic peak was shifted to less values on rising the scan rate from 50–100 mV/s, confirming the irreversible nature of the electrochemical oxidation step [35].

The cyclic voltammograms (CVs) of DCS at various scan rates were further studied to assign the transport features

(adsorption and diffusion) at GCE. On raising the scan rate ( $\nu$ ), the  $i_{p,a}$  steadily increased, and the plots of  $i_{p,a}$  vs. square root of the scan rate ( $\nu^{1/2}$ ) at various known concentrations ( $5.0 \times 10^{-4}$ ,  $1.0 \times 10^{-3}$  and  $2.0 \times 10^{-3}$  M) of DCS were slightly linear (Figure 4(a)). The plots passed through the point of origin revealing the irreversible nature of the electrochemical oxidation process, adsorption-diffusion-controlled process, and the existence of slow chemical reactions in addition to partial mass transfer following the electrode process [35–37]. The anodic peak current significantly increased from the baseline on continuous scan, suggesting passivation of the surface of the GCE electrode via formation of polymeric oxidation products or fouling of the GCE electrode by the produced oxidation products as reported [38,39]. The observed decrease in the  $i_{p,a}$  is most likely attributed to prior adsorption of the analyte on the surface of the non-well-polished GCE surface [35].

The plot of  $\log i_{p,a}$  vs.  $\log \nu$  at pH 2 at GCE vs. Ag/AgCl was linear at the employed scan rates (Figure 4(b)). The plot can be defined by the following linear regression equation:

$$\log i_{p,a} = 0.76 \log \nu - 0.76 \quad (R^2 = 0.9916). \quad (2)$$

The slope (0.76) of the linear plot was greater than 0.5 ( $R^2 = 0.9916$ ), adding further support to the irreversible nature of the electrode process. This value (0.76) of the slope is far from the theoretically value (1.0) expected when there is an adsorption process on the electrode surface [35]. Thus, the electrochemical oxidation of DCS more likely involves a combination of adsorption/diffusion controlled since the slope lies between 0.5 and 1.0 [40].

Diagnostics of the type of the electrode mechanism of the electrochemical oxidation step of conversion of the hydroxyl group (-C-OH) to the corresponding carbonyl (-C=O) group are of prime importance. Thus, the current function ( $i_{p,a}/\nu^{1/2}$ ) was critically studied at various scan rates. The function  $i_{p,a}/\nu^{1/2}$  continuously increased on growing the scan rate, and the plot of the function of  $i_{p,a}/\nu^{1/2}$  at 0.42 V vs. the scan rate at 0.42 V shown in Figure 4 C was nonlinear. Thus, the electrode process most likely favors EE type electrode mechanism, and the electron transfer process is coupled with an irreversible electrochemical step in a rapid follow-up charge transfer as reported [37–39]. The electrochemical oxidation step involves two consecutive oxidation steps involving  $2 H^+/2e$  as demonstrated in Scheme 1, where the rate constant of the electrode process is fast [32, 41–44].

Based on the CV data of DCS at various scan rates at pH 2, the plot of  $\log \nu$  versus  $E_{p,a}$  is demonstrated in Figure 4(d). On growing the scan rate, the anodic peak potential was shifted to more positive value and the plot of  $E_{p,a}$  vs.  $\log \nu$  was linear (Figure 4(d)) revealing the irreversible nature of the electrode process [45–47]. The plot can be defined by this regression equation:

$$E_{p,c} (V) = -133 \log \nu (V \cdot s^{-1}) + 586.5; R^2 = 0.9871. \quad (3)$$

Based on the impact of the scan rate on potential-potential separation ( $\Delta E_p$ ) and the irreversible nature of the electrode process, the data were further subjected to Laviron [48]:



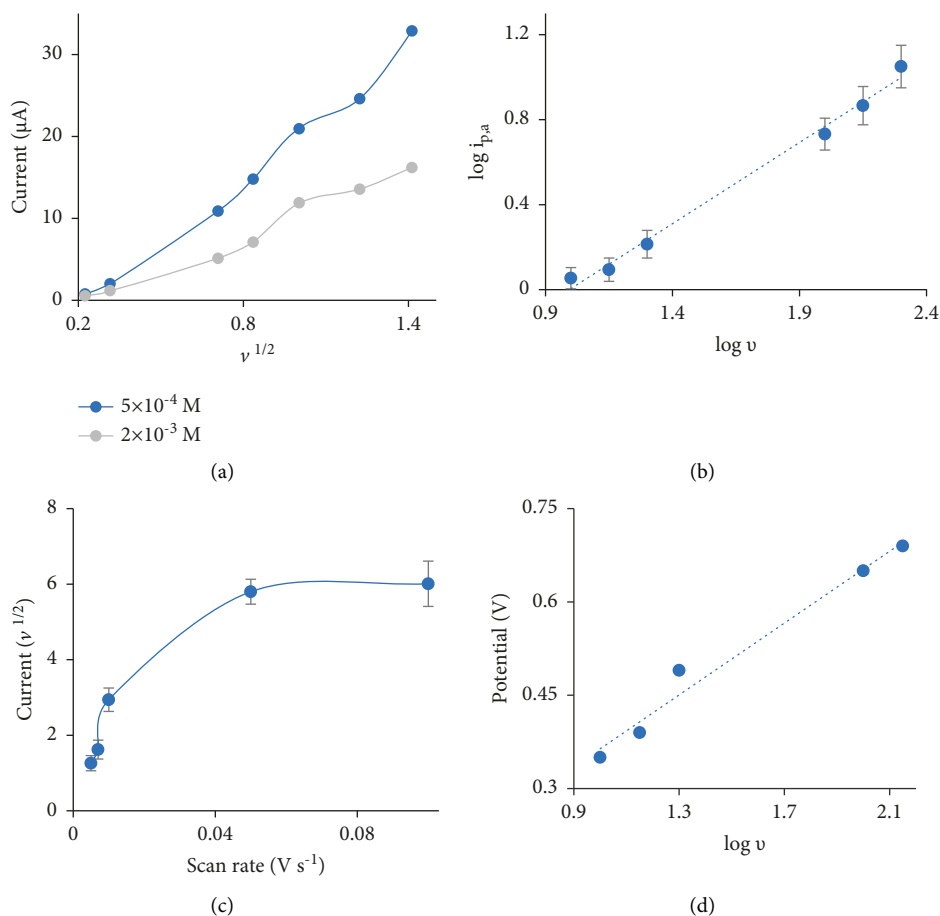


FIGURE 4: Plots of the anodic peak current ( $i_{p,a}$ ) at 0.4 V of DCS  $1.5 \times 10^{-4} \text{ (M)}$  vs. square root of scan rate ( $v^{1/2}$ ) at different concentrations (a);  $\log i_{p,a}$  of DCS vs.  $\log v$  (b); Current function ( $i_{p,a}/v^{1/2}$ ) vs. scan rate (c) and anodic peak potential ( $E_{p,a}$ ) vs.  $\log v$  (d) in B-R buffer (pH $\approx$ 2) at GCE vs. Ag/AgCl electrode using cyclic voltammetry.

reproducible and symmetric anodic peak was observed at 0.40 V vs. Ag/AgCl electrode. The observed decrease in the anodic peak current at pH > 2 is most likely attributed to the formation of unstable electrochemical species and/or formation of polymeric  $\text{-C=O}$  compounds of the DCS.

The influence of the accumulation time (1.0–110 s) on the anodic stripping peak current of the DCS at pH 2–3 using DP-ASV mode was critically studied at 0.07 V deposition potential under stirring (Figure 5(a)). Maximum peak current and well defined anodic peak were noticed at a deposition time of 5 s at  $E_{p,a} = 40 \text{ V}$  vs. Ag/AgCl electrode reveals the strong affinity of the bare GCE towards DCS drug. The anodic peak current at longer accumulation time began to decrease suggesting that the electrode surface was saturated with the DCS steroid. The reason of this behavior is not known, and this trend is most likely a characteristic feature of adsorptive stripping with the stirred solution. Hence, an accumulation time of 5 s was adopted in the subsequent work for DCS determination.

The impact of the deposition potential (0.0–0.35 V) on the anodic peak current of DCS was evaluated vs. Ag/AgCl electrode at the optimized parameters of accumulation time (5 s) and solution pH 2–3 using B-R buffer. Representative data are illustrated in Figure 5(b), where the maximum

anodic peak current was achieved at 7 mV deposition potential; thus, a deposition potential of 7 mV was selected in the next study.

Pulse amplitude and scan rate are the most important parameters that control the shape and reproducibility of the redox reaction in stripping voltammetry. Thus, the impact of the pulse amplitude (0.05–0.1 V) and scan rate (0.02–0.1 V/s) on the Ads DP-ASV anodic peak current of DCS at 0.4 V was studied. Representative results of the impact of pulse amplitude are shown in Figure 5(c). On raising the pulse amplitude up to 0.08 V and scan rate, the anodic peak current increased. Moreover, a sharp and symmetric oxidation peak was achieved at a pulse amplitude of 0.05–0.080 V and at a scan rate less than 0.06 V/s. At a pulse amplitude higher than 0.08 V and 0.06 V/s scan rate, the peak symmetry decreased and became broad because of the increase in the capacitive current. Thus, in the next study, a pulse amplitude of 0.07 V was chosen.

**3.3. Performance Characteristics of the Established Assay.** Under the optimal parameters, the DP-ASVs of DCS at a wide range of known DCS concentrations were recorded. The plot of  $i_{p,a}$  at 0.40 V of the DP-ASVs vs. DCS concentration is

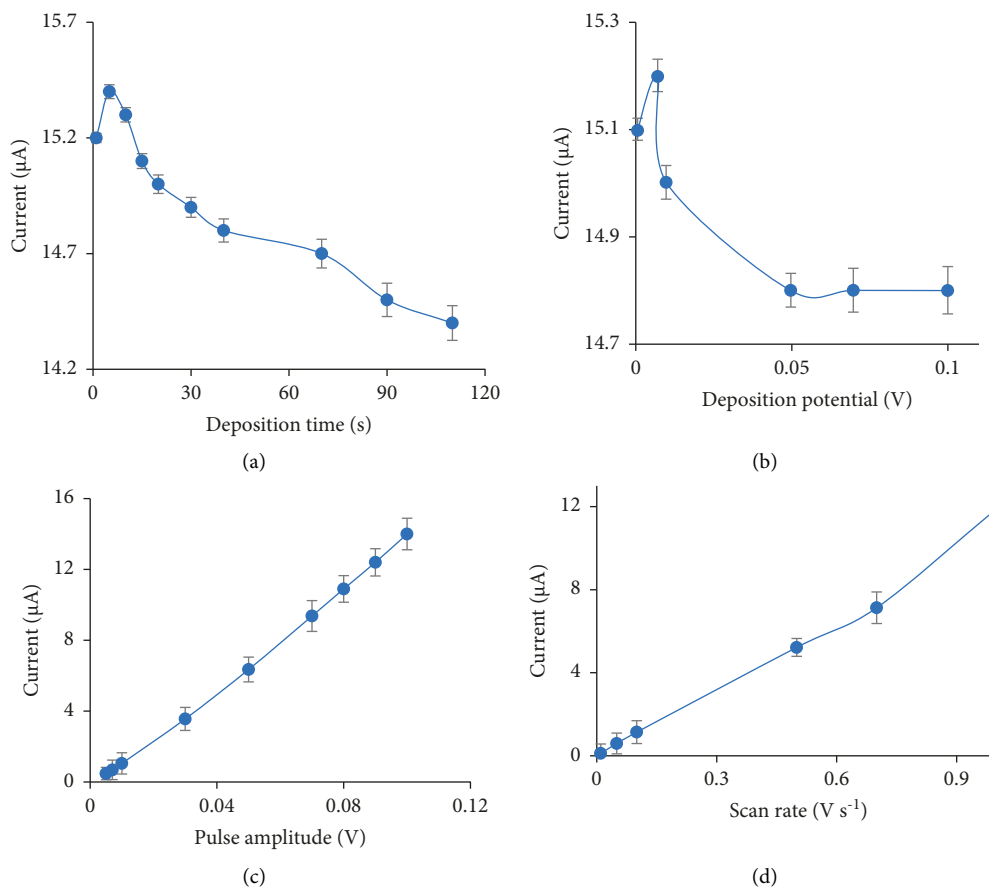


FIGURE 5: Influence of the accumulation time (a), deposition potential (b), pulse amplitude (c), and scan rate (d) on the Ads-DP-ASVs anodic peak current of DCS (10 nM) steroid at GCE vs. Ag/AgCl electrode at  $100 \text{ mVs}^{-1}$  scan rate; 7 mV deposition potential of 0.007 V; pulse amplitude of 70 mV and BR solution of  $\text{pH} \approx 2$ .

shown in Figure 6. The  $i_{p,a}$  at 0.40 V increased linearly over the DCS concentrations in the linear dynamic range 2.5–13.19 nM ( $0.83\text{--}4.36 \text{ ng mL}^{-1}$ ) and leveled off at higher DCS concentration because of the saturation of the DCS species adsorbed DCS at GCE [38, 39]. The linear plot of  $i_{p,a}$  vs. DCS concentration can be described by the following regression equation:

$$i_{p,a} (\mu\text{A}) = 0.6634C (\mu \cdot \text{molL}^{-1}) + 3.3922 \quad R^2 = 0.986. \quad (6)$$

The computed values of low limits of detection ( $\text{LOD} = \text{LOD} = (3\delta)/b$ ) and quantification ( $\text{LOQ} = (10\delta)/b$ ) were calculated [49], where  $\delta$  is the standard deviation of five measurements ( $n = 5$ ), and  $b$  is the slope of the standard plot (it is the sensitivity factor) of the DCS at the optimized variables. The values of LOD and LOQ were found equal to  $9.3 \times 10^{-1} \text{ nM}$  ( $3.1 \times 10^{-1} \text{ ng mL}^{-1}$ ) and 3.1 nM ( $1.02 \text{ ng mL}^{-1}$ ), respectively, at the optimized variables.

A comparison between the performance (LOD, LOQ, and LDR) of the established DP-ASVs method with many reported methods is given in Table 1 [50–53]. It is obvious that the developed probe displays good sensitivity compared with other methods. Moreover, the developed probe is low cost (without metal nanoparticles, e.g., Au, Ag, and Pt), and simple and no prior settings are needed. The LOD of the

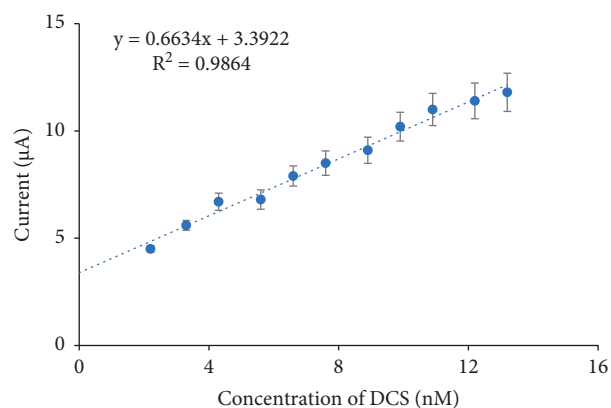


FIGURE 6: Calibration plot of Ads-DP-ASVs of DCS at different concentrations (2.5–13.19 nM) at GCE vs. Ag/AgCl electrode. Sweep rate =  $100 \text{ mVs}^{-1}$ , 5 s accumulation time, 70 mV pulse amplitude and 0.07 V deposition potential at  $\text{pH} \approx 2$  of B-R buffer solution.

developed probe is also lower than the permissible limit of anabolic steroids set by WHO in drinking water. The developed probe also has fast response, no need for high sophisticated instrument, useable, easy for use, and limited

TABLE 1: Comparison between the analytical features of the established DP-ASV and some of the published chromatographic and electrochemical methods\*.

Technique	LDR (ng mL <sup>-1</sup> )	LOD (ng mL <sup>-1</sup> )	Sample	Found level (ng mL <sup>-1</sup> )	Ref
UHPLC-MS/MS	—	1	Mice blood	22	47
LC/MC	—	3 × 10 <sup>-3</sup>	Bird's feather	0.3	48
GC/MS	0.001–10	0.1	Mouse plasma	17.66 ± 9.56	49
Sweeping-MEKC	10–1000	5	Mouse plasma	43	50
DP-ASV-GCE	0.83–4.36	0.73	Tap water	0.87 ± 0.128	Present work

\*Sweeping-MEKC = sweeping-micellar electrokinetic chromatography.

usage of organic reagents and solvents as compared with some of the reported methods (see Table 1). However, the need of GCE for a renewal to every measurement to take away the adsorbed DCS species from the surface of the GCE is the only limitation of the established probe. The validation and precision of the established probe, intraday (repeatability of five measurements in one day) and interday (reproducibility, within 5 days) determination variability, were critically studied. The percent relative standard deviation (% RSD,  $n = 5$ ) of DCS (4.0 ng mL<sup>-1</sup>) at 0.4 V lies between 0.8 and 8.2% supporting the precision of the established assay.

**3.4. Robustness.** The developed method was also tested at minor variations in the pH and deposition time. So, the established DP-ASVs were recorded at pH around pH2-3. The results showed insignificant change ( $\leq 5$  percentage) in the anodic peak current. With slight changes in the deposition time (5–10 s), acceptable values of RSD were also achieved.

**3.5. Selectivity.** The impact of some diverse species in environmental water on the DCS determination by the established DP-ASV was studied. The tolerance limit is defined as the concentration of the added interfering ion creating  $\pm 5\%$  deviation of the anodic peak current at 0.40 V of the aqueous solution of DCS ( $3.3 \times 10^{-8}$  M) at the optimized parameters. The discrimination of the DP-ASV at 0.40 V procedure was applied for the determination of known concentration ( $3.3 \times 10^{-8}$  M) of DCS at mass concentration excess (100-fold) of Na<sup>+</sup>, Co<sup>2+</sup>, Cu<sup>2+</sup>, Fe<sup>2+</sup>, Mn<sup>2+</sup>, Cl<sup>-</sup>, NO<sub>3</sub><sup>-</sup>, Br<sup>-</sup>, CN<sup>-</sup>, NO<sub>2</sub><sup>-</sup>, S<sup>2-</sup>, SO<sub>4</sub><sup>2-</sup> over DCS concentration. Negligible interferences of these ions were achieved. The impact of surface-active agents, e.g., SDS, CITAB, and Triton-100, on the established Ads DPV for DCS determination was also studied, and constancy of the anodic peak current within  $\pm 5\%$  with slight shift in the anodic peak potential ( $\pm 0.05$  V) was noticed, revealing no interference of the tested surface-active agents. Thus, the established assay revealed good discernment towards DCS in the occurrence of usually encountered ionic species and surfactant.

**3.6. Analytical Applications and Validation of the Established Methodology.** Analysis of DCS residues in tap water sample was performed by the established DP-ASV method as described in Section 2.3 using the standards addition method at the optimal conditions. The results are given in Table 2 and the corresponding standard addition plot is shown in ESI. 2.

TABLE 2: Analytical results for determination of DCS in tap water sample by the developed sensor.

Added concentration (ng mL <sup>-1</sup> )	Found concentration (ng mL <sup>-1</sup> )	Recovery (%)
0	0.87 ± 0.128	—
2.2	2.30 ± 0.04	104.5 ± 1.82
3.3	2.89 ± 0.07	87.57 ± 2.12

The “added,” “found,” and recovery percentage (87.57 ± 2.12–104.5 ± 1.82%) of the DCS concentrations were found comparable and acceptable. The DCS concentration of DCS measured was 0.87 ± 0.128 ng/L in agreement with the added value revealing the suitability and precision of the established assay in water samples. Satisfactory recovery (89.7–96.4%) and linearity support the use of the planned methodology for detection of the DCS drug residues in water at trace levels. The experimental Student  $t$  values ( $t_{\text{exp}} = 1.96$ –2.1) were lower than theoretical Student  $t$  value ( $t_{\text{tab}} = 2.78$ ) at  $P < 0.05$  [49], supporting the suitability and versatility of the established sensor. Thus, the planned assay offered suitable precision and accuracy for the drug residues in water samples.

## 4. Conclusion, Advantages, Limitations, and Future Perspectives

The present study reports the analytical utility of DP-ASV at bare GCE for detection of trace levels of DCS residues in water. The proposed assay offered LOD less than the allowable level of DCS in water as set by US- EPA and WHO. The proposed method offered low cost, simple approach, and short analytical time for malathion determination, whereas most of the reported methods suffered from many limitations such as time consuming and use of chlorinated toxic and costly organic solvents. This assay can be improved by combining with dispersive liquid-liquid microextraction techniques and/or modified GCE with nanosized materials, e.g., Ag, Au, and metal oxide as new dimension for ultra-DCS determination. The method can also be employed for DCS residues at trace levels in water samples by online enrichment from large samples volumes of water onto dispersive  $\mu$ -nanosized microextractor (d-  $\mu$ -SPME) packed column prior its determination. This will help in extending the measurable range of target analytes in environmental samples. The current methodology has also the potential to be automated for determination of ultra-trace levels of DCS in biological fluids and environmental water samples *via*

online preconcentration. Experimental design is highly commended, since the one issue at a time has many disadvantages. The interactive effect of various analytical parameters variations might also improve the sign and the application to real samples.

### Data Availability

The data underlying in this study are included in the article and electronic supplementary information, and all are available for readers.

### Ethical Approval

This article does not contain any studies with human participants or animals performed by any of the authors.

### Disclosure

No potential conflicts of interest were reported by the authors.

### Conflicts of Interest

The authors declare that they have no conflicts of interest or personal relationships that could have appeared to influence the work reported in this paper.

### Authors' Contributions

W.T. Alsaggaf did the methodology, writing, and review and editing, as well as funding acquisition. M.S. El-Shahawi did the methodology, validation, formal analysis, investigation, conceptualization, writing, and review and editing.

### Acknowledgments

This project was funded by the Deanship of Scientific Research (DSR) at King Abdulaziz University, Jeddah, under Grant no. G-22-247-39. The authors, therefore, acknowledge with thanks SABIC and DSR for technical and financial support. The research was performed as part of the employment of the author Mohammad El-Shahawi, with the employer King Abdul-Aziz University, Jeddah, KSA.

### Supplementary Materials

(1) chemical structure of 11-desoxycorticosterone; (2) standard addition plot of 11-desoxycorticosterone at different concentrations of DCS at GCE vs. Ag/AgCl electrode. Accumulation time=5 s, pulse amplitude = 0.07 V in B-R buffer (pH = 2-3). (*Supplementary Materials*)

### References

- [1] G. Francis, Z. Kerem, H. P. S. Makkar, and K. Becker, "The biological action of saponins in animal systems: a review," *British Journal of Nutrition*, vol. 88, no. 6, pp. 587–605, 2002.
- [2] E. Olesti, J. Boccard, G. Visconti, V. González-Ruiz, and S. Rudaz, "From a single steroid to the steroidome: trends and analytical challenges," *The Journal of Steroid Biochemistry and Molecular Biology*, vol. 206, Article ID 105797, 2021.
- [3] W. C. Duane, "Bile acids: developments new and very old," *Journal of Lipid Research*, vol. 50, no. 8, pp. 1507–1508, 2009.
- [4] F. Hartgens and H. Kuipers, "Effects of androgenic-anabolic steroids in athletes," *Sports Medicine*, vol. 34, no. 8, pp. 513–554, 2004.
- [5] M. D. Altschule and K. J. Tillotson, "The use of testosterone in the treatment of depressions," *New England Journal of Medicine*, vol. 239, no. 27, pp. 1036–1038, 1948.
- [6] I. Sinha-Hikim, J. Artaza, L. Woodhouse et al., "Testosterone-induced increase in muscle size in healthy young men is associated with muscle fiber hypertrophy," *AJP Endocrinology and Metabolism*, vol. 283, p. 154, 2002.
- [7] S. Bhasin, T. W. Storer, M. Javanbakht et al., "Testosterone replacement and resistance exercise in HIV-infected men with weight loss and low testosterone levels," *JAMA*, vol. 283, no. 6, p. 763, 2000.
- [8] P. Kintz, L. Gheddar, and J. S. Raul, "Simultaneous testing for anabolic steroids in human hair specimens collected from various anatomic locations has several advantages when compared with the standard head hair analysis," *Drug Testing and Analysis*, vol. 13, no. 7, pp. 1445–1451, 2021.
- [9] M. Jauset-Rubio, M. L. Botero, V. Skouridou et al., "One-pot SELEX: identification of specific aptamers against diverse steroid targets in one selection," *ACS Omega*, vol. 4, no. 23, pp. 20188–20196, 2019.
- [10] G. Kanayama, K. J. Brower, R. I. Hudson, and H. G. Pope Jr., "Anabolic-androgenic steroid dependence: an emerging disorder," *Addiction*, vol. 104, no. 12, pp. 1966–1978, 2009.
- [11] J. Boccard, F. Badoud, E. Grata et al., "A steroidomic approach for biomarkers discovery in doping control," *Forensic Science International*, vol. 213, no. 1–3, pp. 85–94, 2011.
- [12] A. Esquivel, É. Alechaga, N. Monfort et al., "Evaluation of sulfate metabolites as markers of intramuscular testosterone administration in Caucasian and Asian populations," *Drug Testing and Analysis*, vol. 11, no. 8, pp. 1218–1230, 2019.
- [13] P. Kintz, "A new series of hair test results involving anabolic steroids," *Toxicologie Analytique et Clinique*, vol. 29, no. 3, p. 320, 2017.
- [14] A. T. Kicman and D. B. Gower, "Anabolic steroids in sport: biochemical, clinical and analytical perspectives," *Annals of Clinical Biochemistry: International Journal of Laboratory Medicine*, vol. 40, no. 4, pp. 321–356, 2003.
- [15] M. Svobodová, V. Skouridou, M. L. Botero et al., "The characterization and validation of 17 $\beta$ -estradiol binding aptamers," *The Journal of Steroid Biochemistry and Molecular Biology*, vol. 167, p. 14, 2017.
- [16] V. Skouridou, M. Jauset-Rubio, P. Ballester et al., "Selection and characterization of DNA aptamers against the steroid testosterone," *Microchimica Acta*, vol. 184, no. 6, pp. 1631–1639, 2017.
- [17] V. Skouridou, T. Schubert, A. S. Bashammakh, M. S. El-Shahawi, A. O. Alyoubi, and C. K. O'Sullivan, "Aptatope mapping of the binding site of a progesterone aptamer on the steroid ring structure analytical," *Biochemistry*, vol. 531, p. 8, 2017.
- [18] S. A. Bhawani, O. Sulaiman, Z. A. Khan, R. Hashim, and M. N. M. Ibrahim, "Resolution of a five-component mixture of quaternary ammonium surfactants on silica gel 60 F 254 high performance thin layer chromatographic plates," *Journal of Surfactants and Detergents*, vol. 14, no. 2, pp. 301–305, 2010.
- [19] H. Liu, T. Lin, X. Cheng, N. Li, L. Wang, and Q. Li, "Simultaneous determination of anabolic steroids and  $\beta$ -agonists

- in milk by QuEChERS and ultra high performance liquid chromatography tandem mass spectrometry,” *Journal of Chromatography B*, vol. 1043, pp. 176–186, 2017.
- [20] Y. Jiafeng, S. Decheng, L. Xiaoyong, L. Yang, L. Guangyu, and B. S. Min, “Multi residue determination of 19 anabolic steroids in animal oil using enhanced matrix removal lipid cleanup and ultrahigh performance liquid chromatography-tandem mass spectrometry,” *Analytical Methods*, vol. 13, no. 21, p. 2374, 2021.
- [21] L. De Wilde, K. Roels, P. Van Renterghem, P. Van Eenoo, and K. Deventer, “Steroid profiling in urine of intact glucuronidated and sulfated steroids using liquid chromatography-mass spectrometry,” *Journal of Chromatography A*, vol. 1624, Article ID 461231, 2020.
- [22] F. Badoud, J. Boccard, C. Schweizer, F. Pralong, M. Saugy, and N. Baume, “Profiling of steroid metabolites after transdermal and oral administration of testosterone by ultra-high pressure liquid chromatography coupled to quadrupole time-of-flight mass spectrometry,” *The Journal of Steroid Biochemistry and Molecular Biology*, vol. 138, pp. 222–235, 2013.
- [23] C. L. Xu, X. G. Chu, C. F. Peng, Z. Y. Jin, and L. Y. Wang, “Development of a faster determination of 10 anabolic steroids residues in animal muscle tissues by liquid chromatography tandem mass spectrometry,” *Journal of Pharmaceutical and Biomedical Analysis*, vol. 41, no. 2, pp. 616–621, 2006.
- [24] A. Esquivel, É. Alechaga, N. Monfort, and R. Ventura, “Direct quantitation of endogenous steroid sulfates in human urine by liquid chromatography-electrospray tandem mass spectrometry,” *Drug Testing and Analysis*, vol. 10, no. 11-12, pp. 1734–1743, 2018.
- [25] P. Van Eenoo, W. Van Gansbeke, N. De Brabanter, K. Deventer, and F. T. Delbeke, “A fast, comprehensive screening method for doping agents in urine by gas chromatography-triple quadrupole mass spectrometry,” *Journal of Chromatography A*, vol. 1218, no. 21, pp. 3306–3316, 2011.
- [26] L. Hintikka, M. Haapala, T. Kuuranne, A. Leinonen, and R. Kostiaainen, “Analysis of anabolic steroids in urine by gas chromatography-microchip atmospheric pressure photoionization-mass spectrometry with chlorobenzene as dopant,” *Journal of Chromatography A*, vol. 1312, pp. 111–117, 2013.
- [27] R. L. Gomes, W. Meredith, C. E. Snape, and M. A. Sephton, “Analysis of conjugated steroid androgens: deconjugation, derivatisation and associated issues,” *Journal of Pharmaceutical and Biomedical Analysis*, vol. 49, no. 5, pp. 1133–1140, 2009.
- [28] N. Jadon, R. Jain, S. Sharma, and K. Singh, “Recent trends in electrochemical sensors for multianalyte detection - a review,” *Talanta*, vol. 161, pp. 894–916, 2016.
- [29] S. K. Yadav, P. Chandra, R. N. Goyal, and Y.-B. Shim, “Chromatography-based determination of anabolic steroids in biological fluids: future prospects using electrochemistry and miniaturized microchip device,” *Chromatographia*, vol. 76, no. 21-22, pp. 1439–1448, 2013.
- [30] L. Huml, J. Tauchen, S. Rimpelová, B. Holubová, O. Lapčík, and M. Jurásek, “Advances in the determination of anabolic-androgenic steroids: from standard practices to tailor-designed multidisciplinary approaches,” *Sensors*, vol. 22, no. 4, pp. 1–29, 2022.
- [31] A. Afkhami, H. Ghaedi, T. Madrakian, D. Nematollahi, and B. Mokhtari, “Electro-oxidation and voltammetric determination of oxymetholone in the presence of mestanolone using glassy carbon electrode modified with carbon nanotubes,” *Talanta*, vol. 121, pp. 1–8, 2014.
- [32] N. M. Alourfi, G. I. Mohammed, H. M. Nassef et al., “A highly sensitive modified glassy carbon electrode with a carboxylated multi-walled carbon nanotubes/naion nano composite for voltammetric sensing of dianabol in biological fluid,” *Analytical Sciences*, vol. 37, no. 12, pp. 1795–1802, 2021.
- [33] N. Terui, B. Fugetsu, and S. Tanaka, “Voltammetric behavior and determination of 17.BETA.-Estradiol at multi-wall carbon nanotube-naion modified glassy carbon electrode,” *Analytical Sciences*, vol. 22, no. 6, pp. 895–898, 2006.
- [34] R. Jain, D. S. Dhanjai, and S. Sharma, “Bismuth (III) oxide/glassy carbon sensor for sensing of antidepressant drug escitalopram in micellar media,” *Colloids and Surfaces A: Physicochemical and Engineering Aspects*, vol. 436, pp. 178–184, 2013.
- [35] K. Scott, “2-electrochemical principles and characterization of bioelectrochemical systems,” *Microbial Electrochemical and Fuel Cells: Fundamentals & Applications*, pp. 29–66, 2016.
- [36] H. T. S. Britton, *Hydrogen Ion*, Chapman & Hall, London, UK, 4th edition, 1952.
- [37] P. Protti, *Introduction to Voltammetric and Polarographic Analysis Technologies*, AMEL, Belgium, 4th edition, 2001.
- [38] K. Peeters, *Tetrakisulphonated phthalocyanine thin films deposited on gold electrodes: a study using voltammetry and synchrotron micro X-Ray fluorescence*, Ph.D thesis, University of Gent, Ghent, Belgium, 2001.
- [39] A. J. Bard and L. R. Faulkner, *Electrochemical Methods, Fundamental and Applications*, John Wiley & Sons, Hoboken, NJ, USA, 2nd edition, 2000.
- [40] R. Wada, S. Takahashi, and H. Muguruma, “New perspective on ECE mechanism of monohydroxycinnamic acid oxidation with carbon nanotube electrode,” *Electrochimica Acta*, vol. 359, Article ID 136964, 2020.
- [41] A. Manjaoui, J. Haladjian, and P. Bianco, “Electrochemical properties of pyrolytic graphite electrodes modified through adsorbed proteins,” *Electrochimica Acta*, vol. 35, no. 1, pp. 177–185, 1990.
- [42] D. T. Sawyer, J. M. Beebe, P. T. Kissinger, and W. R. Heineman, *Chemistry Experiments for Instrumental Methods*, John Wiley & Sons, Hoboken, NJ, USA, 1984.
- [43] H. Lund and O. Hammerich, *Organic Electrochemistry*, Marcel Dekker, New York, 4th edition, 2001.
- [44] K. Raghu, A. Chandrasekar, and K. R. Sankaran, “Electrochemical behavior and differential pulse voltametric determination of an antineoplastic drug bicalutamide and pharmaceuticals formulations using glassy carbon electrode,” *International Journal of Chemical Research*, vol. 2, no. 2, pp. 5–16, 2010.
- [45] B. S. P. Costa, A. C. G. Baró, and E. J. Baran, “Electrochemical and spectroscopic studies of Co(CREATININE)<sub>2</sub>Cl<sub>2</sub>,” *Journal of Coordination Chemistry*, vol. 55, no. 9, pp. 1009–1019, 2002.
- [46] M. S. El-Shahawi and N. H. Khraibah, “Development of a highly sensitive voltametric sensor for trace determination of melamine residues in milk and water samples,” *Microchemical Journal*, vol. 157, Article ID 105087, 2020.
- [47] G. I. Mohammed, N. H. Khraibah, A. S. Bashammakh, and M. S. El-Shahawi, “Electrochemical sensor for trace determination of timolol maleate drug in real samples and drug residues using Nafion/carboxylated-MWCNTs nanocomposite modified glassy carbon electrode,” *Microchemical Journal*, vol. 143, pp. 474–483, 2018.
- [48] E. Laviron, “General expression of the linear potential sweep voltammogram in the case of diffusionless electrochemical

- systems,” *Journal of Electroanalytical Chemistry and Interfacial Electrochemistry*, vol. 101, no. 1, pp. 19–28, 1979.
- [49] J. Miller and N. Miller, *Statistics for Analytical Chemistry*, Ellis-Horwood, New York, 4th edition, 1994.
- [50] M. S.-S. Bergh, I. L. Bogen, J. M. Andersen, Å. M. L. Berg, and T. Berga, “Determination of adrenaline, noradrenaline and corticosterone in rodent blood by ion pair reversed phase UHPLC-MS/MS,” *Journal of Chromatography B*, vol. 1072, pp. 161–172, 2018.
- [51] Z. Bílková, M. Adámková, T. Albrecht, and Z. Šimek, “Determination of testosterone and corticosterone in feathers using liquid chromatography-mass spectrometry,” *Journal of Chromatography A*, vol. 1590, pp. 96–103, 2019.
- [52] P.-Y. Shu, S.-H. Chou, and C.-H. Lin, “Determination of corticosterone in rat and mouse plasma by gas chromatography-selected ion monitoring mass spectrometry,” *Journal of Chromatography B*, vol. 783, no. 1, pp. 93–101, 2003.
- [53] C.-H. Wu, M.-C. Chen, A.-K. Su, P.-Y. Shu, S.-H. Chou, and C.-H. Lin, “Determination of corticosterone in mouse plasma by a sweeping technique using micellar electrokinetic chromatography,” *Journal of Chromatography B*, vol. 785, no. 2, pp. 317–325, 2003.